Core–Shell Nanoparticles

DOI: 10.1002/ange.200602559

Diffusion of Gold into InAs Nanocrystals**

*Taleb Mokari, Assaf Aharoni, Inna Popov, and Uri Banin**

Multicomponent nanoparticles are at the forefront of research into nanomaterials.[1–5] The combination of a metal and a semiconductor in the same nanoparticle is of particular interest as the metal can provide an anchor point for electrical and chemical connections to the functional semiconductor part. This possibility was demonstrated recently by the growth of gold tips on the apexes of CdSe nanorods to form nano-dumbbells,[6] where at a high Au-to-rod concentration a transition from two- to one-sided growth occurs.[7] Au was also recently grown on lead chalcogenide nanoparticles, leading to segregated portions of the metal and semiconductor.[8] Au has been found to undergo surface diffusion between neighboring wires at moderate temperatures on Si nanowires grown by a vapor–liquid–solid method with Au as catalyst.[9,10] Herein we

[*] T. Mokari, A. Aharoni, Dr. I. Popov, Prof. U. Banin
Department of Physical Chemistry and
Center for Nanoscience and Nanotechnology
The Hebrew University of Jerusalem
Jerusalem 91904 (Israel)
Fax: (+972) 2-658-4148
E-mail: banin@chem.ch.huji.ac.il

[**] We thank Professor Ulrich Gösele for helpful discussions. This research was supported in part by the EU-FP6 program under project SA-NANO, and by the US–Israel bi-national science foundation (BSF). T.M. thanks the Ministry of Science, Israel, for an Eshkol Fellowship.

report a completely different behavior in the room-temperature reaction of Au with InAs nanoparticles. In this case, Au diffuses into the InAs particles to give a Au core coated by an amorphous shell.

The diffusion of metals into semiconductors has been studied extensively for bulk materials[11,12] because this process has significant relevance for the processing of integrated electronic circuits. Indeed, solid-state diffusion, which is typically carried out at high temperatures, is used extensively in their fabrication. Low-temperature reactions and diffusion have been detected for various metal–semiconductor pairs such as Au-Si and Au with binary semiconductors. Hiraki, for example, has found that low-temperature reaction and diffusion of the metals generally occurs when the semiconductor band-gap energy (E_g) is lower than about 2.5 eV and the dielectric constant $\varepsilon > 8$.[13] The diffusion properties of the specific metal also determine the possibility of room-temperature diffusion into the semiconductor. Metals that show such room-temperature diffusion are classified as "fast" diffusers,[14] and diffusion coefficient of these metals is larger than the self-diffusion coefficient.

Fast diffusion in semiconductors covers a wide range of different mechanisms. Among these, the interstitial-substitutional mechanisms are of interest here. The most important mechanisms that have been studied and proposed for fast diffusers (impurities) incorporated in semiconductors are:[15] 1) host interstitial mediated diffusion, also known as the "kick-out" mechanism,[16] in which atoms move rather rapidly by a direct interstitial mechanism until they eventually displace a lattice atom, and 2) the "Frank–Turnbull" mechanism,[16,17] which initiates at a vacancy in the host. In this case the impurity atom does not dislodge the lattice atom but becomes trapped in a vacancy, thereby becoming almost immobile. These mechanisms occur in numerous systems, including metals in III–V semiconductors (that is, where III is an element from Group III of the periodic table and V is an element from Group V), diffusion of elements into silicon and germanium, and probably also in II–VI compounds.

Diffusion into nanoparticles was recently used to form hollow particles by taking advantage of the "Kirkendall effect",[18] in which pores form because of the difference in diffusion rates between two components in a diffusion couple.[19] Room-temperature diffusion is also involved in ion-exchange reactions that lead to the transformation of nanoparticle composition, for example, from CdSe to Ag_2Se.[20] These recent examples show the richness of the possible routes for performing chemistry in nanoparticles and herein we provide another example concerning the diffusion of gold into InAs nanocrystals at room temperature.

The diffusion coefficient can be expressed in an Arrhenius form [Equation (1)] where D_0 is the pre-exponential factor and E_a is the activation energy.

$$D = D_0 \, e^{(-E_a/RT)} \tag{1}$$

Typically, these values are measured at high temperature[21] and therefore room-temperature values can be obtained only by extrapolation. An estimate for the typical diffusion distance with time is given by the root-mean-square (RMS) distance (X), which is given by Equation (2).

$$X = \sqrt{2\,D\,T} \tag{2}$$

The reaction of Au with InAs nanoparticles is similar to our earlier synthesis of Au-CdSe nano-dumbbells.[6] It was carried out at room temperature by adding an $AuCl_3$ solution to InAs dots dissolved in toluene. The gold solution contains the gold salt, didodecyldimethylammonium bromide (DDAB, to bring the Au salt into the organic solution), and dodecylamine (DDA), which stabilizes the dots and serves as a reducing agent (see Experimental Section for details). Figure 1 shows TEM images of InAs dots after reaction

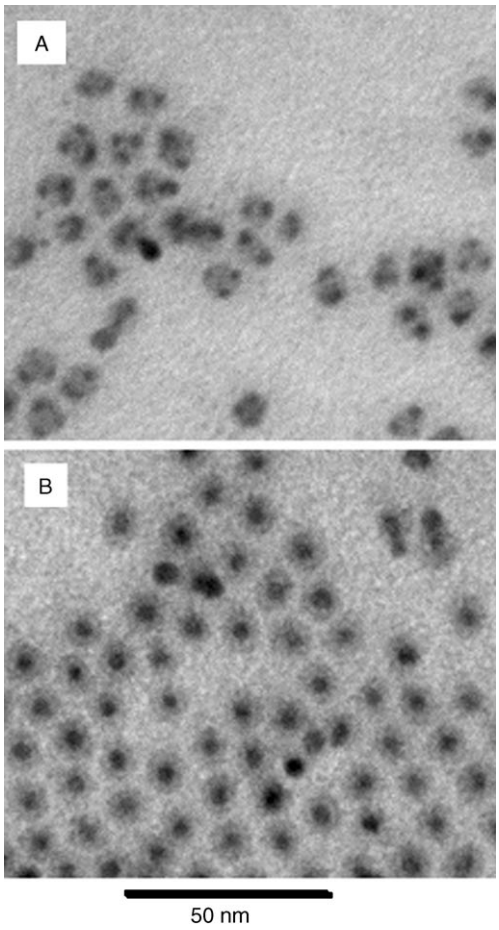

Figure 1. TEM images of InAs nanocrystals after treatment with gold in toluene solution as a function of increasing gold concentration: A) after adding 2.75×10^{-6} mol of gold; B) after adding 5.5×10^{-6} mol of gold. Reaction time: 2 min.

with Au. At a low concentration of Au (Figure 1 A), Au patches are formed on the InAs surface, as can be seen by the dark spots. Upon doubling the Au concentration a completely different behavior is seen: the Au diffuses to the center of the nanoparticle and is coated with a shell with much lower contrast in the TEM image. This behavior is in contrast to that observed for the reaction of Au with CdSe nanoparticles, where gold grows in patches on the surface (or on the apexes

of rods), and at high concentrations transforms into one patch (or one side for rods) through a ripening process.

Optical and structural characterization of the Au-InAs system was carried out by various methods. Figure 2A presents the absorption spectra of the original InAs dots (7-nm diameter) before and after their reaction with gold; note that the excitonic peak of the InAs dots has been washed out. Figure 2B shows the powder X-ray diffraction (XRD) pattern acquired from the original 7-nm InAs dots before the Au growth (Figure 2B, top), which agrees with the zincblende structure of bulk crystalline InAs (peak positions are represented by the upper stick-spectrum). The XRD pattern of the Au-InAs composite (Figure 2B, bottom) is also shown. In this pattern, we can identify three peaks attributed to Au, with the (111) peak being especially strong. The fourth, broad diffraction peak (marked by an arrow) can be attributed to the (222) planes of zincblende-type In_2O_3 (see the stick pattern at the bottom of Figure 2B). Thus, no evidence of the presence of crystalline InAs appears in the XRD pattern of the Au-InAs nanocomposite. By comparing the diffraction results for InAs nanodots and the Au-InAs nanocomposite we can therefore conclude that the latter material is less ordered.

The energy-dispersive X-ray spectrum of the Au-InAs nanocomposite is shown in Figure 2C. In addition to the In and the As from the original core, a Au peak appears for the Au-InAs system. Quantification of this spectrum resulted in an In/As/Au ratio of 0.89:0.83:1.

The Au-InAs nanocomposite was also studied by high-resolution TEM (HRTEM) measurements (Figure 3). These gave a lattice spacing in the dark core of 2.35 Å, which agrees with the (111) lattice spacing of Au. This Au lattice was identified in the center of many particles. Studying the shell proved difficult owing to the low contrast, which differs significantly from the core. However, by focusing on the shell of the composite particles we were able to find evidence for an average lattice spacing of 2.95 Å (10 particles), which may indicate the presence of (111) planes of In_2O_3, as shown in Figure 3B.

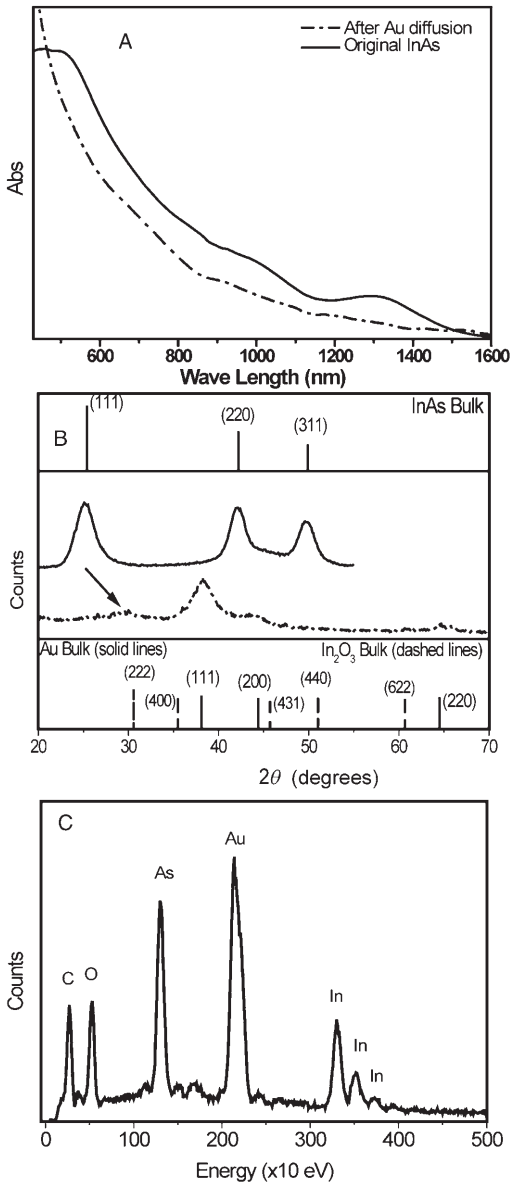

Figure 2. Optical and structural characterization of the Au-InAs nanocomposite: A) absorption spectra of 7-nm InAs dots before (solid line) and after reaction with Au (dashed line); B) powder XRD patterns of InAs (top) and Au-InAs (bottom) and the stick-patterns of bulk InAs (top), gold, and In_2O_3; arrow indicates peak assigned to the (222) planes of zincblende-type In_2O_3; C) EDS spectrum of the Au-InAs nanocomposite.

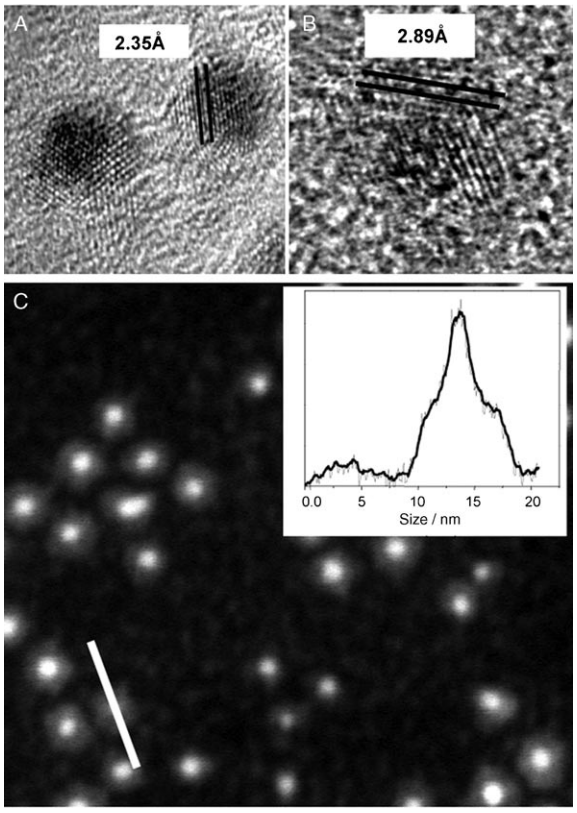

Figure 3. Structural characterization of Au-InAs particles: A) HRTEM image of two particles; the measured lattice spacing in the core is 2.35 Å; B) HRTEM image of the particle taken by focusing on the shell; the measured lattice spacing is 2.89 Å. C) STEM-HAADF image of *Z*-contrast observed in several particles. The intensity distribution across a single particle (white line) is presented in the inset.

To further study the structure of the Au-InAs nanocomposite, we used the scanning transmission electron microscopy (STEM) technique with a high angular annular dark-field detector (HAADF). The integrated intensity of the signal is proportional to the average atomic number of the sampled elements (Z-contrast imaging). Figure 3C shows an STEM-HAADF image of the nanocomposite. A significant contrast difference between the core and the shell, where the bright core indicates the presence of the heavier Au component, can be seen for the particles. This feature can also be seen in the inset, which shows a cross-section of a single particle taken along the marked line. A main peak is observed with two weaker shoulders corresponding to the shell.

The role of solid-state diffusion in the creation of the Au-InAs particles was emphasized by performing a reaction in the solid state. Thus, after adding 1×10^{-6} mol of Au solution to the InAs solution (similar to the solution experiment), an aliquot was taken and deposited on the TEM grid. The results show a typical behavior for this specific concentration with gold patches on the surface (Figure 4A). The same grid was stored and examined again 48 h later, thereby allowing for further reaction to proceed. The TEM image in Figure 4B clearly shows that the gold has diffused inside to yield a result very similar to that obtained in solution for a high Au concentration.

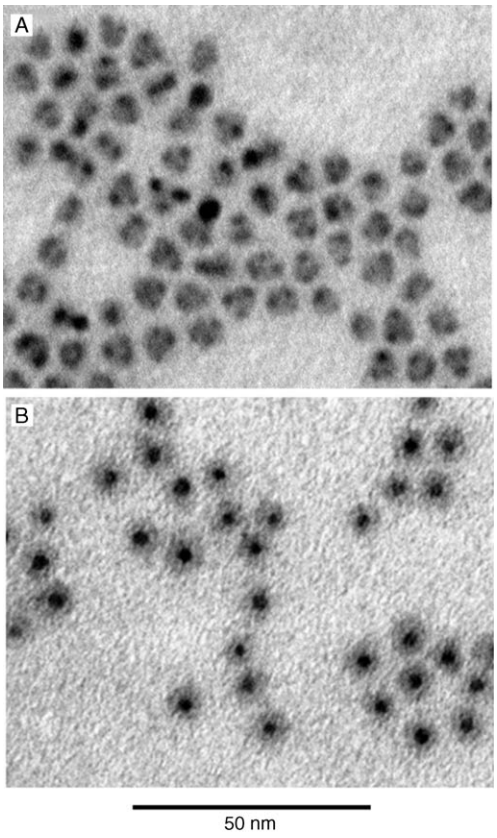

Figure 4. TEM images of gold diffused inside InAs nanocrystals as a function of time. 1×10^{-6} mol of gold was added and an aliquot was deposited on the TEM grid and characterized after 2 h (A) and 48 h (B). The reaction time in solution was 2 min.

This latter experiment resembles classical diffusion studies in bulk materials, where metal films are deposited on a substrate and heated up and the diffusion is monitored by measuring the metal concentration profile inside the bulk material, although in the bulk these experiments are performed at very high temperature.[11,15]

Our observations clearly show that Au diffuses into the InAs dots. During this diffusion, the InAs loses its crystalline order and becomes an amorphous shell (under inert conditions), while In is converted into In_2O_3 in the oxidizing environment. To examine the feasibility of such room-temperature diffusion, we used Equation (1) to estimate the diffusion coefficient (D) for Au in InAs at room temperature. A value of about $3 \times 10^{-14}\,m^2 s^{-1}$ was obtained. From Equation (2) we calculated approximately that the RMS diffusion distance, X, will be around 1000 nm in 24 h. This diffusion behavior differs significantly from that observed in CdSe dots, where Au forms patches on the surface that ripen to one patch at high Au concentration. We could not determine D values for Au in CdSe, but for the similar system of Au in CdS, D at room temperature is much smaller, approximately $1 \times 10^{-29}\,m^2 s^{-1}$, and correspondingly X over 24 h is negligible (approximately 2×10^{-5} nm). Much smaller values were also calculated for the CdTe system. The main difference is the much lower activation energy in the Au-InAs case (0.65 eV versus 1.8 eV for Au in CdS and 2 eV for Au in CdTe).[21] The diffusion of Au into InAs also agrees with the criteria for room-temperature diffusion of fast diffusers as the InAs dots have an energy gap of 1.1 eV and the dielectric constant is high (14.2 for InAs).

The detailed diffusion behavior in this case can be attributed to an interstitial-substitution mechanism.[16,17] This diffusion process is indeed a typical solid-state reaction and can also take place on the grid in the absence of solvent. The gold atoms hop from the surface into the nanoparticles through the interstitial sites of the InAs nanocrystal and simultaneously substitute atoms of the InAs lattice. Free In and As atoms simultaneously diffuse out and may be readily oxidized in the absence of an inert atmosphere. Migrating interstitial gold atoms distort the atomic lattice of the hosting InAs nanocrystal because these atoms are still relatively large for interstitial positions, even for the 6.058-Å unit cell of InAs. Therefore, the mass substitution of In atoms at high Au concentrations results in the formation of an amorphous shell.

The diffusion process does not lead to a homogeneous distribution of Au across the particle. Rather, Au is concentrated in the center of the nanoparticles. This arrangement is probably due to the preferred strong interaction between the Au atoms. The original InAs nanocrystals with a size of 7 nm should be composed of roughly 20 atomic planes of the (111) type (d-spacing of 3.498 Å), which means that only 10 interatomic jumps are required for a migrating gold atom to get to a core position within the InAs particle. On the other hand, the gold content in the Au-InAs nanocomposite reaches a level of 30% atomic concentration, which apparently determines the minimum-energy geometry of the composite as a dense, compact gold core ($19\,g\,cm^{-3}$; about 2 nm in size) surrounded by an amorphous InAs shell instead of an amorphous particle containing a mixture of Au, In, and As atoms with a density

close to 5.7 $g\,cm^{-3}$, as for the InAs crystal, and a size larger than that of the original InAs nanodots.

To summarize, the diffusion of gold into InAs semiconductor nanocrystals has been reported. The diffusion of Au occurs either in solution or in a solid-state reaction. In the first stage gold patches grow on the nanocrystal surface, and a further increase in the gold concentration, or waiting for 24 h, leads to gold diffusion into the nanocrystals. This behavior differs from the CdSe case, where Au grows on the surface and ripens to form one gold patch in high concentration. As a result of the Au diffusion, the InAs is converted into an amorphous InAs or oxidized shell. This process points to a new strategy for metal doping in semiconductor nanoparticles.[22]

Experimental Section

The InAs nanocrystals were prepared as reported elsewhere.[23,24]

In a typical reaction, a gold solution was prepared from $AuCl_3$ (2.5 mg, 0.008 mmol), DDAB (20 mg, 0.04 mmol), and DDA (35 mg, 0.185 mmol) in toluene (4 mL) and sonicated for 5 min at room temperature. The solution changed color from dark orange to light yellow. InAs quantum dots (0.8 mg, 2.35×10^{-10} mol of dots) were dissolved in toluene (5 mL) in a three-necked flask under argon and the gold solution was added dropwise at room temperature. During the addition, the color gradually changed to dark brown. Separation of the Au-InAs product from the growth solution was performed by adding of methanol (1 mL), which leads to precipitation, and centrifuging for 5 min.

TEM images were obtained with a FEI Tecnai 12 microscope or a FEI Tecnai F20G^2 microscope operating at 200 kV. Energy-dispersive X-ray spectroscopy (EDS) was carried out with a 5-kV acceleration voltage on an HR SEM FEI Sirion equipped with an EDAX EDS detector. Powder XRD patterns were measured with a Philips PW 1830/40 X-ray diffractometer with $Cu_{K\alpha}$ radiation. Absorption measurements were taken with a Jasco UV-VIS-NIR spectrophotometer.

Received: June 27, 2006
Revised: August 29, 2006
Published online: November 2, 2006

Keywords: core–shell nanoparticles · gold · materials science · solid-phase synthesis

[1] D. J. Milliron, S. M. Hughes, Y. Cui, L. Manna, J. Li, L. W. Wang, A. P. Alivisatos, *Nature* **2004**, *430*, 190 – 195.
[2] S. Kudera, L. Carbone, M. F. Casula, R. Cingolani, A. Falqui, E. Snoeck, W. J. Parak, L. Manna, *Nano Lett.* **2005**, *5*, 445 – 449.
[3] D. V. Talapin, R. Koeppe, S. Gotzinger, A. Kornowski, J. M. Lupton, A. L. Rogach, O. Benson, J. Feldmann, H. Weller, *Nano Lett.* **2003**, *3*, 1677 – 1681.
[4] T. Teranishi Y. Inoue, M. Nakaya, Y. Oumi, T. Sano, *J. Am. Chem. Soc.* **2004**, *126*, 9914 – 9915.
[5] H. Yu, M. Chen, P. M. Rice, S. X. Wang, R. L. White, S. Sun, *Nano Lett.* **2005**. *5*, 379 – 382.
[6] T. Mokari, E. Rothenberg, I. Popov, R. Costi, U. Banin, *Science* **2004**, *304*, 1787 – 1791.
[7] T. Mokari, C. G. Sztrum, A. Salant, E. Rabani, U. Banin, *Nat. Mater.* **2005**, *4*, 855 – 862.
[8] W. Shi, H. Zeng, Y. Sahoo, T. Y. Ohulchanskyy, Y. Ding, Z. L. Wang, M. Swihart, P. N. Prasad, *Nano Lett.* **2006**, *6*, 875 – 881.
[9] J. B. Hannon, S. Kodambaka, F. M. Ross, R. M. Tromp, *Nature* **2006**, *440*, 69 – 71.
[10] U. Gösele, *Nature* **2006**, *440*, 34 – 35.
[11] A. F. W. Willoughby, *Rep. Prog. Phys.* **1978**, *41*, 1665 – 1705.
[12] U. Gösele, *Annu. Rev. Mater. Sci.* **1988**, *18*, 257 – 282.
[13] A. Hiraki, *Surf. Sci. Rep.* **1984**, *3*, 357 – 412.
[14] A. Seeger, K. P. Chik, *Phys. Status Solidi B* **1968**, *29*, 455 – 542.
[15] D. Mathiot, *Phys. Rev. B* **1992**, *45*, 13345 – 13355.
[16] U. Gösele, W. Frank, A. Seeger, *Appl. Phys.* **1980**, *23*, 361 – 368.
[17] F. C. Frank, D. Turnbull, *Phys. Rev.* **1956**, *104*, 617 – 618.
[18] A. D. Smigelskas, E. O. Kirkendall, *Trans. AIME* **1947**, *171*, 130 – 142.
[19] Y. Yin, R. M. Rioux, C. K. Erdonmez, S. Hughes, G. A. Somorjai, A. P. Alivisatos, *Science* **2004**, *304*, 711 – 714.
[20] D. H. Son, S. M. Hughes, Y. Yin, A. P. Alivisatos, *Science* **2004**, *306*, 1009 – 1012.
[21] M. B. Dutt, B. L. Sharma in *Diffusion in Semiconductors and Non-Metallic Solids* (Ed.: D. L. Beke), Springer, Berlin, **1998**, pp. 1 – 3.
[22] S. C. Erwin, L. Zu, M. I. Haftel, A. L. Efros, T. A. Kennedy, D. J. Norris, *Nature* **2005**, *436*, 91 – 94.
[23] A. A. Guzelian, U. Banin, A. V. Kadavanich, X. Peng, A. P. Alivisatos, *Appl. Phys. Lett.* **1996**, *69*, 1432 – 1434.
[24] A. Aharoni, T. Mokari, I. Popov, U. Banin, *J. Am. Chem. Soc.* **2006**, *128*, 257 – 264.

